EurJOC
European Journal
of Organic Chemistry

FULL PAPER

A *peri*-Cyclised Naphthalene Dimer: Synthesis and Properties of an Unusual Vilsmeier–Haack Product of 1,3,6,8-Tetramethoxynaphthalene

Michael Pittelkow,*[a] Christian B. Nielsen,[a] Theis Brock-Nannestad,[a] Magnus Schau-Magnussen,[a] and Jørn B. Christensen*[a]

An unusual *peri*-dimerised product was obtained when subjecting 1,3,6,8-tetramethoxynaphthalene to Vilsmeier–Haack reaction conditions (POCl$_3$/DMF). The formation of this *peri*-dimerised naphthalene product suggests that 1,3,6,8-tetramethoxynaphthalene has comparable reactivity to that of Proton Sponge [1,8-bis(dimethylamino)naphthalene]. The octamethoxy *peri*-dimer was characterised using NMR spectroscopy, mass spectrometry, UV/Vis spectroscopy, Raman spectroscopy, electrochemistry, X-ray crystallography and DFT calculations. The one-electron oxidation of the *peri*-dimerised naphthalene compound yielded a radical cation that was studied by EPR spectroscopy and UV/Vis spectroscopy at low temperatures. The experimental observations were confirmed by DFT calculations.

Introduction

The 1- and 8-positions in naphthalenes are *peri* (literally meaning "near") to each other.[1,2] Two substituents in *peri* positions are (for most functional groups) located in closer proximity to each other than are substituents in *ortho* positions. The *peri* positions in naphthalenes are the simplest example of a *peri* region in polycyclic aromatic hydrocarbons (PAHs), making it the most obvious system to study to understand the reactivity of larger PAHs. Balasubramaniyan recognised that steric strain due to bulky substitution at interfering positions can be relieved in a number of ways, including stretching of bonds, in-plane deflection of the substituents, out-of-plane deflection of the substituents, and distortion or buckling of the naphthalene nucleus.[1] When designing materials based on naphthalenes (or larger PAHs), the *peri*-effect must be taken into consideration to account for factors that seem straightforward when designing materials based on benzene.[3] Overcrowding has a profound influence on the properties of materials based on PAHs, and issues such as planarity of the aromatic core, reactivity, and substituent effects are less trivial than for benzene-based materials.[4]

In elegant work by Pozharskii and co-workers on the substitution of 1,8-bis(dimethylamino)naphthalene (Proton Sponge) by various electrophilic reagents, some unusual products have been described (Figure 1).[5] Electron-donating substituents placed in strategic positions on naphthalene cores are particularly effective in the stabilisation of naphthylmethyl carbocations (especially in the α-position). An example of such substituents would be the 1,8-bis(dimethylamino) groups in Proton Sponge. The formation of stable benzyl-like carbocations in the vicinity of very electron-rich aromatic cores may give rise to electrophilic aromatic substitution reactions. Some of the unusual *peri*-cyclised structures isolated by Pozharskii and co-workers are shown in Figure 1.
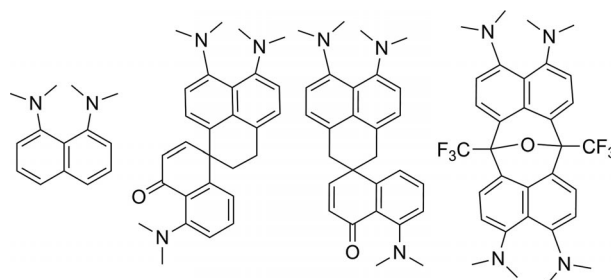

Figure 1. Proton Sponge [1,8-bis(dimethylamino)naphthalene] and *peri*-cyclised structures.

In a recent study, we have used DFT calculations to predict the energy requirements for the formation of various methoxy-substituted naphthylmethyl carbocations.[6] These calculations showed that the energy requirements for the formation of the carbocation are sensitive to a number of factors, such as substitution pattern, planarity of the aromatic core, and the *peri*-effect. The most pronounced destabilising effect proved to be overcrowding of the periphery of the aromatic core, which forced the substituents out of the aromatic plane, thus interrupting the conjugation.

[a] Department of Chemistry, University of Copenhagen, Universitetsparken 5, 2100 Copenhagen Ø, Denmark
E-mail: pittel@kiku.dk
jbc@kiku.dk

WILEY ONLINE LIBRARY

FULL PAPER

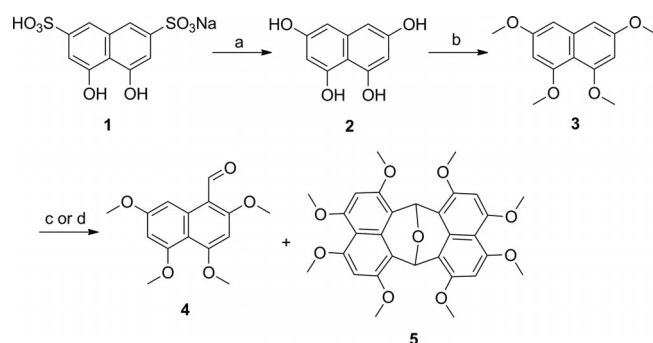M. Pittelkow, J. B. Christensen et al.

These computational considerations indicated that a 2,4,5,7-tetramethoxy-1-naphthylmethyl carbocation would be the most stable methoxy-substituted naphthylmethyl carbocation.

In this paper, we show that the introduction of four methoxy substituents in such a way as to avoid over-crowding of the periphery of the naphthalene core results in an effect on the reactivity of the aromatic core comparable to that arising from the introduction of the *peri*-bis(dimethyl-amino) substituents in Proton Sponge. Furthermore, we show that the dimeric naphthalene compound formed is a potent donor molecule in which the two naphthalene moieties interact with each other through space.

Synthesis

Tetrahydroxynaphthalene (**2**) was prepared in 56% yield by modifying the procedure of Tanaka et al.[7] Thus, chromotropic acid sodium salt (**1**) was heated with a mixture of $Ba(OH)_{2(s)}$, $KOH_{(s)}$, and $NaOH_{(s)}$ to 250 °C under a flow of N_2 overnight. Tetramethylation proceeded to completion upon heating an acetone suspension of the tetrahydroxy compound with excess dimethyl sulfate and K_2CO_3 for 48 h (85%). It was found to be more convenient to methylate the crude 1,3,6,8-tetrahydroxynaphthalene to yield 1,3,6,8-tetramethoxynaphthalene (**3**).[8]

The transformation of 1,3,6,8-tetramethoxynaphthalene (**3**) into aldehyde **4** using a Vilsmeier–Haack formylation ($POCl_3$ in DMF) proved to be highly dependent on concentration, temperature and reaction time (Scheme 1).[8,9] At temperatures below –10 °C, no reaction occurred, and only when allowing the reaction mixture to heat up slowly to –5 °C did the formylation reaction take place. When performing this reaction under relatively dilute conditions (0.03 M) at –5 °C, aldehyde **4** was isolated as a single isomer in moderate yield (52%) after 2 h. When scaling this reaction up to gram scale, we carried out the reaction in a more concentrated solution (0.16 M), and the reaction mixture was stirred at room temperature overnight. This resulted in a disappointing 2% yield of the aldehyde and the formation of another compound as the major product (**5**, 65%). When

performing NMR spectroscopy, the compound was sensitive to trace amounts of acid in the $CDCl_3$. The proton NMR spectrum of **5** showed only a few signals, indicating a high degree of symmetry. Mass spectrometry (FAB+) and elemental analysis indicated a dimeric condensation product. We speculate that the mechanism for the formation of **5** is a double electrophilic aromatic substitution reaction at the *peri* positions on opposite molecules. Dehydration and cyclisation would give the locked polycyclic molecule.

X-ray Crystallographic Analysis

Upon crystallisation by slow concentration of a solution of **5** in a 1:1 mixture of CH_3CN/heptane, two distinct crystal morphologies of the same compound appeared: one consisting of white plates (**5a**, with heptane, Figure 2) and one consisting of white octahedral crystals (**5b**, with MeCN, Figure 3). The structure of **5** was confirmed to be a product
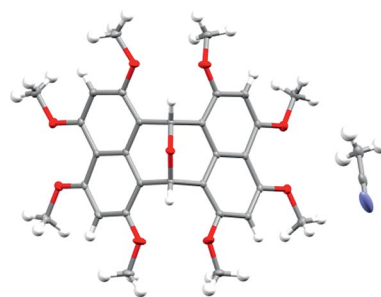

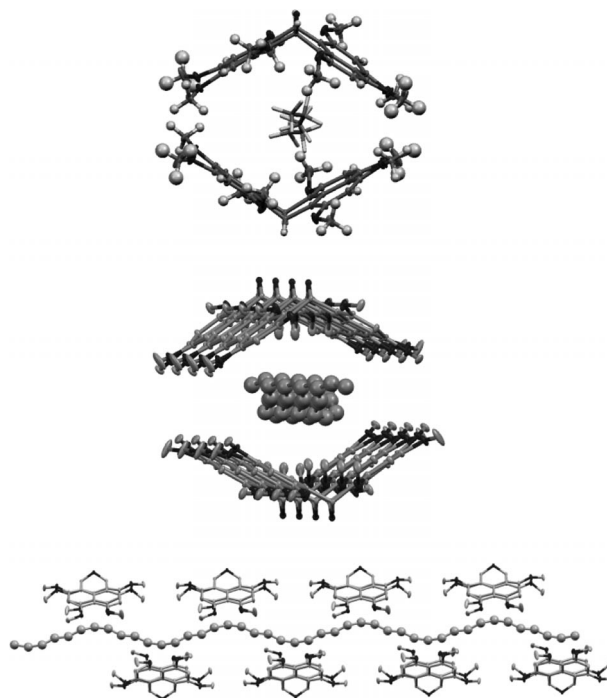Figure 2. X-ray crystal structure of MeCN-solvated compound **5b**.

Figure 3. Views of the X-ray crystal structure of the heptane-solvated crystals of **5a** showing the chains of alkane surrounded by molecules of **5**.

Scheme 1. Reagents and conditions: (a) $Ba(OH)_2$·$8H_2O$, KOH, NaOH, 260 °C, 12 h, 56%; (b) (i) $Ba(OH)_2$·$8H_2O$, KOH, NaOH, 260 °C, 12 h, (ii) Me_2SO_4, acetone, K_2CO_3, 48 h, 60% (two steps); (c) $POCl_3$, DMF, c = 0.03 M, –5 °C, 2 h, 52% (**4**); (d) $POCl_3$, DMF, c = 0.16 M, –5 °C, 24 h, 65% (**5**).

of dimerisation of **4** with the loss of one water molecule. The molecule is highly symmetrical with only two different types of methoxy substituent and only one type of aromatic protons. The two naphthalene moieties are connected through the *peri* positions forming an eight-membered ring. This eight-membered ring is further bridged by an oxygen atom to complete the rigid polycyclic structure of **5**.

When viewing only one molecule of **5**, the angle between the two naphthalene moieties (mean planes) is 111.7°, and all the methoxy groups have their methyl moieties in the plane of the aromatic ring. The coplanarity of the methoxy substituents is a feature that is supported by our computational predictions.[6]

The two different crystal morphologies were a result of co-crystallisation with each of the two crystallisation solvents. In the MeCN-solvated crystal structure, the density of **5** is higher than in the heptane-solvated crystals of **5**. The heptane-solvated crystals are particularly interesting as the disordered chains of heptane are part of an inclusion complex with **5**, as seen in the packing of the crystal structure (Figure 2).

Optical and Vibrational Spectroscopy

In Figure 4, the UV/Vis spectra of 1,3,6,8-tetramethoxynaphthalene (**3**) and dimer **5** in acetonitrile are shown. For **3**, two bands were observed, with vibrational fine structure only being observed for the low-energy band. Fine structure was observed for both of the bands observed in the spectrum of **5**, and a Franck–Condon analysis using the Huang–Rhys approach was carried out for both bands.[10] The purpose of this analysis was to quantify the S_1 energy in order to scrutinise the ability of subsequent DFT calculations to predict the electronic structure of the molecule.
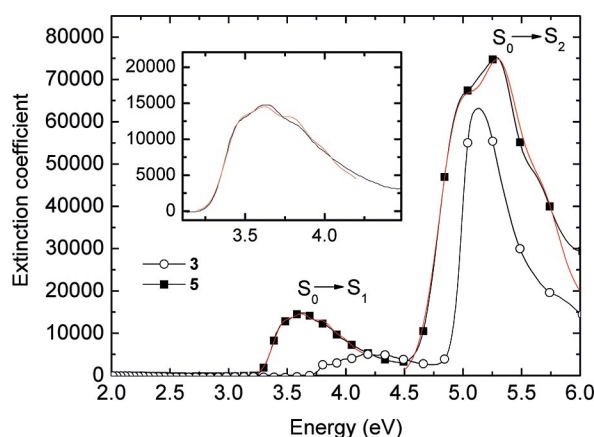

Figure 4. UV/Vis spectra of dimer **5** and 1,3,6,8-tetramethoxynaphthalene (**3**) in MeCN. The red curves are the calculated bands based on the Franck–Condon analysis.

The Franck–Condon/Huang–Rhys analysis was carried according to the following expression,[11]

$$I(\omega) \propto \sum_{n_i} \prod_i \frac{S_i^{n_i} exp\,(-S_i)}{n_i!} exp\left(-\frac{(\omega-\omega_0\pm\sum_i n_i \omega_{p,i})^2}{2\sigma^2}\right),$$

where ω is the frequency, ω_o is electronic origin frequency, ω_p is the phonon frequency, S_i is the Huang–Rhys factor, i is a normal mode in the final state with frequency ω_p, σ is the width of the broadened line at half height for the electronic transition at ω_o, and n_i is the progression of the ith normal mode in the Poisson distribution. The "+" sign is used for analysing absorption spectra and the "–" sign for emission spectra (see Supporting Information).

Two vibrational modes were used to model the fine structure in the absorption band centered around 3.6 eV observed in the spectrum of **5**, whereas only one vibrational mode was used to model the band observed at ca. 5.4 eV. One of the two modes contributing to the low-energy band is actually an overtone of the other. For the phonon energy, we found values of 0.18 eV (1450 cm^{-1}) and 0.39 eV (2981 cm^{-1}), the latter being assigned as an overtone. The corresponding S values are 1.15 and 0.27, respectively. A strong band at 1392 cm^{-1} and a weaker band at 1450 cm^{-1} were found in the Raman spectrum of **5** (see Supporting Information). From the analysis, a value for the energy of the electronic transition $S_0 \rightarrow S_1$ of 3.43 eV was found.

The Franck–Condon analysis of the bands observed in the spectrum of **3** revealed phonon energies of 0.16 and 0.32 eV, with corresponding S values of 1.44 and 0.97, thus an overtone is likely to be contributing to the phonon coupling.[11] Attempts to describe the spectrum with only one vibrational mode were not successful, and including more than two modes did not result in a better fit. Previous work on the photophysics of conjugated polymers has shown that the Huang–Rhys factor for a specific transition decreases when the chain-length is increased. Along with the observation that there is a redshift in the absorption spectra for the lowest-lying states when going from **3** to **5**, this indicates that there is an electronic communication between the two naphthalene rings in **5**.

DFT Calculations

Calculations were performed on **5** using the well-established B3LYP/6-31G(d) level of theory. Initially, a geometry optimisation was carried out, and using this geometry the excitation energies and oscillator strengths for the 30 lowest states were calculated. The results of these calculations are shown in the Supporting Information. In Figure 5, the HOMO and LUMO of **5** are shown, indicating some electronic through-bond communication between the two naphthalene moieties. In particular, in the HOMO–1 and LUMO orbitals, part of the orbitals extends from one naphthalene unit to the other across the eight-membered ring. A single electronic transition governing the low energy of the spectrum was observed with an excitation energy of 3.47 eV, in good agreement with the experimentally observed value.
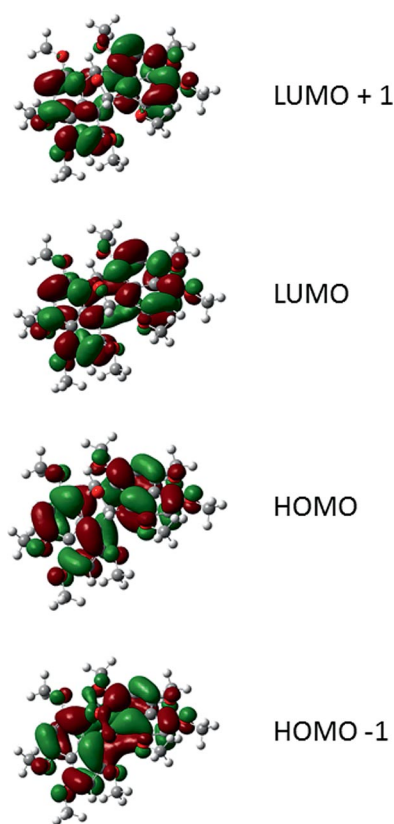
FULL PAPER

M. Pittelkow, J. B. Christensen et al.

Figure 5. Orbital picture for the HOMO–1, HOMO, LUMO and LUMO+1 of the naphthalene dimer **5**.

Figure 6. Top: EPR spectrum of oxidised dimer **5** at 170 K (g = 2.002). Middle and bottom: CV and SW voltammograms of dimer **5** in CH_2Cl_2 with 0.1 M Bu_4NPF_6 as the supporting electrolyte against the Fc/Fc^+ couple. The scan rate was 0.3 V/s.

Electrochemistry and EPR Spectroscopy

Electrochemical measurements of dimer **5** showed two independent oxidations at approximately 0.75 V and 0.86 V against the Fc/Fc^+ couple. In Figure 6, the cyclic voltammogram and the square wave (SW) voltammogram are shown. In the SW voltammogram it is especially clear that the oxidation proceeds in two steps. This indicates that the oxidation of the first naphthalene moiety influences the oxidation of the second naphthalene moiety.

Electrocrystallisation of dimer **5** with Bu_4NPF_6 in CH_2Cl_2 was attempted with approximately 10 µA using a standard setup. The solution turned green, and a dark precipitate was observed. However, no X-ray quality crystals were obtained. Upon chemical oxidation of **5** by addition of $NO^+BF_4^-$ in MeCN to a solution of **5** in CH_2Cl_2, the mixture immediately turned green, but the colour quickly turned yellow/orange. This solution was characterised by UV/Vis spectroscopy and EPR spectroscopy. The UV/Vis spectrum showed a band at 510 nm. The solution was yellow-fluorescent, and MALDI-TOF analysis and TLC analysis of the oxidised solution did not show the presence of the starting material. The yellow/orange species was EPR-silent. During the oxidation, a green colour was observed, and if the oxidation was performed at –78 °C, the green colour persisted for several minutes. This green species was EPR-active, and the EPR spectroscopy was performed in the cold. A solution of **5** in CH_2Cl_2 was frozen
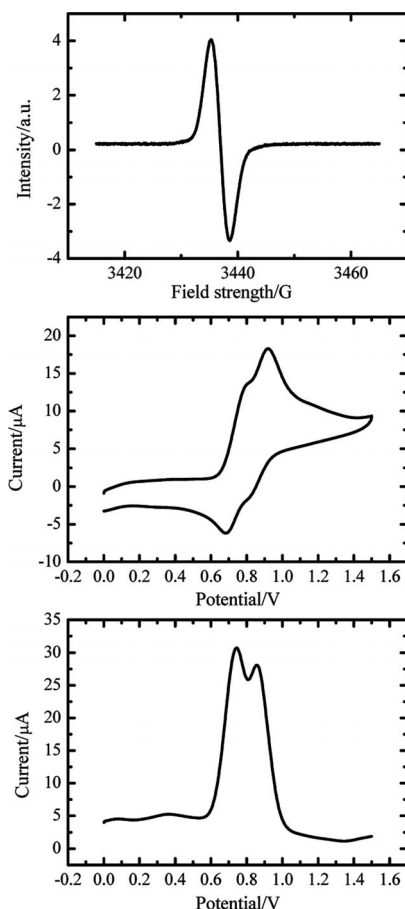
in liquid N_2, and then a solution of the oxidant in MeCN was added and frozen. This mixture was then allowed to warm up and mix in the cooled EPR apparatus, and EPR spectra were recorded at different temperatures. At 70 K, the EPR signal was very weak, but gradual heating of the sample to 170 K gave a convincing EPR signal (Figure 6). The EPR signal corresponds to the mono-oxidised species. Even with an excess of the oxidising agent, the doubly oxidised species was not observed by EPR. A UV/Vis spectrum of the oxidised species was recorded at ca. 195 K, and it showed a band at 642 nm. This band is presumably due to the radical cation.

Conclusions

The formation of a *peri*-cyclised dimeric species of 1,3,6,8-tetramethoxynaphthaldehyde under Vilsmeier–Haack conditions has been observed. The dimer has been characterised by NMR spectroscopy, mass spectrometry, elemental analysis, UV/Vis spectroscopy, fluorescence spectroscopy, Raman spectroscopy, electrochemistry, ESR spectroscopy, and single-crystal X-ray crystallography. The spectroscopic properties have been confirmed by DFT cal-

culations. This dimeric species is formed as a consequence of the electron-rich nature of the aromatic core induced by the four methoxy substituents. These four methoxy substituents affect the reactivity of the aromatic core similarly to how the two *peri*-(dimethylamino) substituents affect the reactivity of Proton Sponge. The two naphthalene moieties communicate, as observed by UV/Vis spectroscopy, and a radical cation is observed by EPR spectroscopy. Donor materials based on electron-rich naphthalene compounds could compliment the properties of other electron-rich aromatic compounds such as TTF, thiophene and alkoxybenzenes. Further studies into the reactivity of these types of compounds are necessary to allow their implementation in materials science.

Experimental Section

General Experimental Procedures: Thin-layer chromatography (TLC) was carried out using aluminium sheets pre-coated with silica gel 60F (Merck 5554). Dry column vacuum chromatography was carried out using silica gel 60 (Merck 9385, 0.015–0.040 mm).[12] Melting points were determined with a Büchi melting point apparatus. ^{1}H NMR (300 MHz) and ^{13}C NMR (75 MHz) spectra were recorded using a Varian instrument. Samples were prepared using deuterated solvents (CDCl$_3$, [D$_6$]DMSO, CD$_2$Cl$_2$) purchased from Cambridge Isotope Labs. Fast atom bombardment (FAB) spectra were obtained with a Jeol JMS-HX 110 tandem mass spectrometer in the positive-ion mode using 3-nitrobenzyl alcohol (NBA) as matrix. EI mass spectra were recorded with a ZAB-EQ (VG-Analytical) instrument. Microanalyses were performed by Mrs. Birgitta Kegel at the Microanalytical Laboratory of the Department of Chemistry, University of Copenhagen. UV/Vis spectra were recorded with a Cary 5E spectrometer (Varian Inc.) with pure solvent as baseline. The Raman spectra were recorded with a Bruker IFS66 NIR-FT instrument equipped with an FRA106 Raman module. An Nd:YAG laser operating at 1064 nm with an output of 300 mW was used as the excitation source. The detector was a Ge diode cooled to liquid-nitrogen temperature. 1,3,6,8-Tetramethoxynaphthalene was synthesised according to ref.[8]

Electron Paramagnetic Resonance Spectroscopy: EPR spectra were recorded using a Bruker Elexsys E-500 instrument equipped with an EIP 538B frequency counter and an ER035M NMR Gauss meter. The EPR spectroscopy was performed in the cold.

X-ray Crystallography: All single-crystal X-ray diffraction data were collected at 122(1) K with a Nonius KappaCCD area-detector diffractometer equipped with an Oxford Cryostreams low-temperature device using graphite-monochromated Mo-K_α radiation ($\lambda = 0.71073$ Å). The structures were solved by direct methods (SHELXS97), and refined using the SHELXL97 software package.[13] All non-hydrogen atoms were refined anisotropically, hydrogen atoms were located in the difference Fourier map and refined isotropically as constraint riding their parent atom in a fixed geometry. The structure of **5a** contains disordered solvent. The packing of **5a** facilitates solvent-accessible channels in which the alkanes of crystallisation are distributed disorderedly. The disorder was modelled by a hexane molecule which by symmetry results in solvent chains running through the structure. Crystal structure and refinement data for **5a** and **5b** are summarised in Table 1. The molecular structure diagrams were made with the ORTEP-3 and Mercury 3.0.1 programs[14] (Figures 2 and 3). CCDC-870028 (for **5a**) and -870029 (for **5b**) contain the supplementary crystallographic data

for this paper. These data can be obtained free of charge from The Cambridge Crystallographic Data Centre via www.ccdc.cam.ac.uk/data_request/cif.

Table 1. X-ray structure and refinement data for **5a** and **5b**.

	5a	**5a**
Empirical formula	C$_{30}$H$_{30}$O$_9$·C$_3$H$_7$	C$_{30}$H$_{30}$O$_9$·0.5C$_2$H$_3$N
Formula mass	577.63	555.07
Crystal system	tetragonal	monoclinic
a [Å]	12.6748(10)	30.9946(7)
b [Å]	12.6748(10)	7.8373(10)
c [Å]	36.6642(19)	21.5701(25)
α [°]	90	90
β [°]	90	99.328(9)
γ [°]	90	90
V [Å^3]	5890.3(7)	5170.2(9)
Temperature [K]	122(1)	122(1)
Space group	$I4_1/2d$	$C2/c$
Z	8	8
Radiation type	Mo-K_α	Mo-K_α
μ [mm^{-1}]	0.094	0.105
No. of reflections measured	95824	74180
No. of independent reflections	6489	8970
R_{int}	0.0721	0.1162
Final R_1 value [$I > 2\sigma(I)$]	0.0605	0.0538
Final $wR(F^2)$ value [$I > 2\sigma(I)$]	0.1590	0.1261
Final R_1 value (all data)	0.0855	0.0866
Final $wR(F^2)$ value (all data)	0.1817	0.1511
Goodness of fit on F^2	1.125	1.090

Calculations: The Gaussian 03 suite of programs was used for the DFT calculations.[15] Initially, geometry optimisations were carried out at the B3LYP/6-31G(d) level of theory, where all the structures were constrained to C_{2v} symmetry. Frequency calculations were then carried out to assure that the structures were indeed minima on the potential energy surface (no imaginary frequencies). TD-DFT calculations and single-point calculations on the anion radicals were then carried out at the B3LYP/6-31G(d) level of theory on these optimised structures. The Gaussian archive entries for these calculations are included in the Supporting Information. GaussView 3.0 was used for generating the orbital plots.

Cyclic Voltammetry: Tetrabutylammonium tetrafluoroborate, Bu$_4$NBF$_4$ (Aldrich, 98%) and acetonitrile, MeCN (Lab-Scan, HPLC grade) were used as received. The cell was a cylindrical vial equipped with a Teflon top with holes to accommodate the Pt working electrode, the Pt counter electrode and the Fc/Fc$^+$ electrode. The electrochemical equipment was from CHI instruments (CH630), with *iR* compensation. The solutions for voltammetry were 1 mm in substrate, and were made by dissolving an accurately weighed amount of the substrate in the required volume of an MeCN/Bu$_4$NBF$_4$ (0.1 m) solution. The volume of the resulting solutions was typically between 5 and 10 mL. The solutions were purged with nitrogen saturated with MeCN for at least 10 min prior to the measurements.

Dimer 5: 1,3,6,8-Tetramethoxynaphthalene (**3**) (1.55 g, 6.24 mmol) was dissolved in anhydrous DMF (40 mL), and the mixture was cooled to –5 °C. POCl$_3$ (1.72 mL, 2.87 g, 18.7 mmol) was added dropwise over 5 min. The reaction mixture was stirred for 30 min at –5 °C, and then water (20 mL) was added, and the reaction mixture was stirred at room temperature for 16 h. The yellow mixture was extracted with CH$_2$Cl$_2$ (6×40 mL), dried (MgSO$_4$), and filtered through paper, and the solvents were evaporated to dryness in vacuo. Dry column vacuum chromatography (heptane to EtOAc with 10% increments) yielded aldehyde **4** as a colourless solid (yield

FULL PAPER

40 mg, 2%) and the dimer **5** as a colourless solid (yield 1.1 g, 65%). M.p. 256–258 °C (decomposition). ^{1}H NMR (CDCl$_3$): δ = 6.83 (s, 2 H), 6.43 (s, 4 H), 3.97 (s, 12 H), 3.91 (s, 12 H) ppm. ^{13}C NMR (CDCl$_3$): δ = 157.5, 153.1, 131.2, 112.5, 108.2, 93.8, 64.5, 56.5, 56.3 ppm. MS (FAB$^+$): m/z = 534.2. HRMS (FAB$^+$): calcd. for C$_{30}$H$_{30}$O$_9$ 534.1890; found 534.1904. C$_{15}$H$_{16}$O$_5$ (276.29): calcd. C 67.41, H 5.66; found C 67.03, H 5.71.

Supporting Information (see footnote on the first page of this article): NMR and Raman spectra, computational data.

Acknowledgments

[1] V. Balasubramaiyan, *Chem. Rev.* **1966**, *66*, 567–641.

[2] V. V. Mezheritskii, V. V. Tkachenko, *Adv. Heterocycl. Chem.* **1990**, *51*, 2–105.

[3] a) U. Boas, J. B. Christensen, K. J. Jensen, *J. Comb. Chem.* **2004**, *6*, 497–503; b) U. Boas, J. Brask, K. J. Jensen, *Chem. Rev.* **2009**, *109*, 2092–2118; c) M. Pittelkow, U. Boas, M. Jessing, K. J. Jensen, J. B. Christensen, *Org. Biomol. Chem.* **2005**, *3*, 508–514.

[4] M. L. Bushey, T. Nguyen, W. Zhang, D. Horoszewski, C. Nuckolls, *Angew. Chem.* **2004**, *116*, 5562; *Angew. Chem. Int. Ed.* **2004**, *43*, 5446–5453.

[5] a) A. F. Pozharskii, N. G. Tregub, N. V. Vistorobskii, E. Y. Romanova, Z. A. Starikova, A. I. Yanovsky, *Russ. Chem. Bull.* **1999**, *48*, 1299–1309; b) A. F. Pozharskii, *Russ. Chem. Rev.* **1998**, *67*, 1–24; c) A. F. Pozharskii, O. V. Ryabtsova, N. V. Vistorobskii, Z. A. Starikova, *Russ. Chem. Bull.* **2000**, *49*, 1097–1102.

[6] M. Pittelkow, J. B. Christensen, T. I. Sølling, *Org. Biomol. Chem.* **2005**, *3*, 2441–2449.

[7] H. Tanaka, Y. Ohne, N. Ogawa, T. Tamura, *Agric. Biol. Chem.* **1963**, *27*, 48.

[8] M. Pittelkow, U. Boas, J. B. Christensen, *Org. Lett.* **2006**, *8*, 5817–5820.

[9] G. Jones, S. P. Stanforth, *Org. React.* **1997**, *49*, 1–330.

[10] K. Kanemoto, T. Sudo, I. Akai, H. Hashimoto, T. Karasawa, Y. Aso, T. Otsubo, *Phys. Rev. B* **2006**, *73*, 235203.

[11] a) M. F. Granville, B. E. Kohler, J. B. Snow, *J. Chem. Phys.* **1981**, *75*, 3765–3769; b) J. Cornil, D. Beljonne, Z. Shuai, T. W. Hagler, I. Campbell, D. D. C. Bradley, J. L. Brédas, C. W. Spangler, K. Müllen, *Chem. Phys. Lett.* **1995**, *247*, 425–432.

[12] D. S. Pedersen, C. Rosenbahm, *Synthesis* **2001**, 2431–2434.

[13] G. M. Sheldrick, *Acta Crystallogr., Sect. A* **2008**, *64*, 112.

[14] a) L. J. Farrugia, *J. Appl. Crystallogr.* **1997**, *30*, 565; b) C. F. Macrae, P. R. Edgington, P. McCabe, E. Pidcock, G. P. Shields, R. Taylor, M. Towler, J. van de Streek, *J. Appl. Crystallogr.* **2006**, *39*, 453.

[15] J. Frisch, G. W. Trucks, H. B. Schlegel, G. E. Scuseria, M. A. Robb, J. R. Cheeseman, V. G. Zakrzewski, J. A. Montgomery, Jr., R. E. Stratmann, J. C. Burant, S. Dapprich, J. M. Millam, A. D. Daniels, K. N. Kudin, M. C. Strain, O. Farkas, J. Tomasi, V. Barone, M. Cossi, R. Cammi, B. Mennucci, C. Pomelli, C. Adamo, S. Clifford, S. J. Ochterski, G. A. Petersson, P. Y. Ayala, Q. Cui, K. Morokuma, D. K. Malick, A. D. Rabuck, K. Raghavachari, J. B. Foresman, J. Cioslowski, J. V. Ortiz, B. B. Stefanov, G. Liu, A. Liashenko, P. Piskorz, I. Komaromi, R. Gomperts, R. L. Martin, D. J. Fox, T. Keith, M. A. Al-Laham, C. Y. Peng, A. Nanayakkara, C. Gonzalez, M. Challacombe, P. M. W. Gill, B. Johnson, W. Chen, M. W. Wong, J. L. Andres, M. Head-Gordon, E. S. Replogle, J. A. Pople, *Gaussian 98*, revision A.11.3, Gaussian Inc, PA, **1998**.

Received: April 21, 2012
Published Online: ■

EurJOC
European Journal
of Organic Chemistry

The Vilsmeier–Haack reaction (POCl$_3$/DMF) of 1,3,6,8-tetramethoxynaphthalene gave an unusual *peri*-cyclised dimer as well as the 1-naphthaldehyde. The dimer is a potent donor molecule.

**M. Pittelkow,* C. B. Nielsen,
T. Brock-Nannestad,
M. Schau-Magnussen,
J. B. Christensen*** **1–7**

A *peri*-Cyclised Naphthalene Dimer: Synthesis and Properties of an Unusual Vilsmeier–Haack Product of 1,3,6,8-Tetramethoxynaphthalene